ANNALS OF PHYSICS: 8, 1–23 (1959)

Melting Properties of He^3 and He^4 up to 3500 kg/cm^2*

E. R. Grilly and R. L. Mills

University of California, Los Alamos Scientific Laboratory, Los Alamos, New Mexico

For He^3 and He^4 the volume change on melting, ΔV_m, the molar volume of fluid, V_f, and the fluid thermal expansion coefficient, $\alpha_f[\equiv(1/V_f)(\partial V_f/\partial T)_P]$, were measured along the melting curve from 1.3 to 31°K at pressures up to 3500 kg/cm². These are the first such measurements to be reported for He^3; for He^4 they are the first measurements, consistent with melting curve determinations, which cover this pressure range accurately. Detailed studies of all the melting parameters were made at pressures below 250 kg/cm² for both isotopes. Two solid forms of He^3 were found with a transition line which intersects the melting curve at 3.15°K and 141 kg/cm². For He^4 an indirect determination was made of the intersection of the lambda line with the melting curve.

I. INTRODUCTION

Although the melting curves of He^3 and He^4 have been traced in considerable detail from a few tenths of a degree absolute up to 30 and 50°K, respectively, (*1–12*) there exist no measurements of the corresponding volume change on melting, ΔV_m, for He^3 and no direct measurements for He^4 above 4°K. Such data in combination with slopes of the melting curves are useful in deriving the various thermodynamic quantities of melting. For He^4, ΔV_m measurements have been made by Swenson (*6, 7, 13*) in the region 1.2 to 4.0°K. In addition there are indirect measurements by Keesom and Keesom (*9*) in the region 2.2 to 4.0°K, and by Dugdale and Simon (*3*) in the region 4 to 26°K. The most precise of these measurements occur below 4°K where the quoted (*6, 7*) error is 3 percent. For He^3 and He^4, ΔV_m data consistent with the melting curve determinations in accuracy and extent (*1*) are especially desirable.

Reported here are final determinations of the volume change on melting of He^3 and He^4 up to 3500 kg cm^2. It should be noted that some preliminary data have already been presented (*14*). This study is part of a continuing program to measure the melting parameters for all the low boiling gases; in the past measurements for N_2 were reported (*15*).

* Work done under the auspices of the U. S. Atomic Energy Commission.

II. EXPERIMENTAL

A. Apparatus

The apparatus was similar to that which has been described elsewhere (*15*). It consisted of an oil hydraulic system in equilibrium with a high-pressure gas system through a mercury U-tube. Gas from the high-pressure system was metered in a low-pressure volume manometer

Incorporated in the hydraulic system were a hand pump, intensifier, oil injector, and free-piston gauge. Two different piston gauges were required to cover the full pressure range. Pressures from 5 to 125 kg/cm^2 were read on a commercial[1] free-piston gauge, whose effective area was determined by balancing the gauge against the known vapor pressure of CO_2 at 0°C (*16*). In the range 50–3500 kg/cm^2, pressures were measured with a controlled-clearance free-piston gauge, previously described in some detail (*1*). At pressures above 200 kg/cm^2, the weights were suspended below the piston by a yoke, rods, and pan. The piston was rotated by the method of Myers and Jessup (*17*). Below 200 kg/cm^2 the weights were placed on a pan above the piston and rotated by hand. Over the region of mutual accessibility, 50 to 125 kg/cm^2, both piston gauges were in agreement. Movement of the pistons was measured either with a height indicator gauge of calibrated spring constant or with a traveling telescope. Readings were reproducible to about 0.01 mm.

In the U-tube which separated the oil system from the gas system, mercury levels were indicated by external magnetic coils which sensed the position of ferritic steel balls floating on the mercury surface inside the nonmagnetic steel columns of the U. The levels could be read to 0.5 mm, and differences in mercury level between the two arms were applied as corrections to the piston pressures.

The gas system was identical to that shown previously (see Fig. 1, Ref. 15) with the exception that in most of the runs below 200 kg/cm^2 Valve 2 was removed and the manganin gauge was relocated between Valves 3 and 4. For all runs, Valves 1 and 3 were replaced by shop-made valves (*18*) which featured unsupported area packings and nonrising spindles for constancy of volume during operation.

Many of the determinations below 250 kg cm^2 were made in a cell different from that already described (*15*). The new low-pressure cell had a nominal volume of 0.4 cm^3 and was made of thin-walled AISI No. 304 stainless steel. Both cells were equipped with inlet capillaries which were vacuum-jacketed. Electrical heaters and thermocouples were spaced along the capillary so that room temperature could be maintained to within several millimeters of the cell opening.

A special gas handling system was required for the rare isotope He^3. The gas

[1] Ashcroft Gauge Tester 1300-25, Manning, Maxwell, and Moore, Inc., Stratford, Connecticut.

was stored below atmospheric pressure in a 12-l tank. It was pumped by a pressure-vacuum, reversible, 2-stage vane pump[2] through a purifying train consisting of a charcoal trap cooled to liquid N_2 temperature and a charcoal trap cooled to liquid H_2 temperature. The gas then entered a cryogenic pump where it was liquefied at $\sim$2°K and 2 kg/cm^2 gauge pressure. Upon warming, the purified high-pressure gas was forced either into the ΔV_m apparatus or into a small compression cylinder for additional pressure boosting. At the completion of an experiment, He^3 in the low-pressure metering system was transferred back to the storage reservoir by the same vane pump. Residual gas at a few microns pressure was removed by a conventional vacuum system. Mass spectrometer analysis of the purified gas indicated the following impurities: 0.06 percent He^4, $<$0.015 percent H_2, $<$0.005 percent D_2, $<$0.005 percent T_2, $<$0.01 percent N_2, $<$0.002 percent O_2.

The source of the He^4 was an A.E.C. cylinder (H size) filled at the Bureau of Mines Amarillo Station. The gas was pressured by a 3-stage compression cylinder and passed through a liquid-N_2 cooled trap into the measuring system. Mass spectrometer analysis indicated the following impurities: 0.01 percent H_2, 0.03 percent N_2, 0.002 percent O_2.

B. General Procedure

The experimental technique used in measuring ΔV_m was essentially the same as that described earlier (*15*). However, the temperatures employed in freezing and melting the sample were, in general, much closer to the equilibrium melting points. This obviated large corrections for the thermal expansion of solid and fluid.

At pressures below 1000 kg/cm^2, the fluid coefficient of thermal expansion α_f was determined by the following piston displacement method. Fluid in the cell was brought to pressure equilibrium with the piston gauge at a cell temperature near the freezing point. A valve was closed, isolating the cell, whereupon the cell temperature was raised $\sim$0.2°K. After temperatures had equilibrated, the valve was opened and the corresponding piston travel in the piston gauge was observed. From known PVT of the gas, the volume change could be computed. This procedure was repeated over several ΔT's at the same pressure and for both warming and cooling. At pressures above 1000 kg cm^2 the earlier technique (*15*) was used.

The fluid compressibility coefficient β_f was measured similarly. At constant temperature the cell was balanced against the piston gauge. The cell valve was closed, an additional weight was added to the piston pan, the valve was opened and the piston displacement observed. At a given temperature the procedure

[2] A brief description of this pump is given by Sydoriak and Roberts (*19*).

was repeated at different ΔP's up to the freezing point. Measurements were also taken for pressure decrements.

For redeterminations of the melting curves below 200 kg cm^2, the apparatus and technique described in a preceding paper (*20*) were employed. Determination of the solid-solid transition line for He^3, however, was carried out in the ΔV_m apparatus as follows. With the He^3 pressure held constant at some value below the triple point, the bath was lowered out of contact with the cell. The bath temperature was then adjusted to a value just below the expected transition line, and the bath level was raised slowly until the cell was about one-half immersed. This filled the lower portion of the cell with solid. The existing temperature gradient in the upper part of the cell kept the cell opening from plugging with solid. With the bath temperature and level held constant, small weights were added stepwise to the piston gauge. The piston dropped by small decrements due to the compressibility of the system until the transition line was reached, at which point an additional weight caused the piston to drop by a large amount corresponding to the volume change of solid-solid transition, ΔV_{trans}, which took place in the lower portion of the cell. Unfortunately the measurement of ΔV_{trans} could not be made quantitative by this method since the exact amount of solid in the cell was indeterminable. A different method for determining ΔV_{trans} is discussed in Section IV-B-1.

The room temperature density of gaseous He^3 and He^4 was measured at three different pressures up to 200 kg/cm^2 by simply emptying an equilibrated cell content into the low-pressure metering system. Fluid density along the melting curve was measured as before (*15*).

The procedures outlined above will, in general, succeed only at temperatures which can be maintained by boiling liquid baths. No attempt was made to obtain ΔV_m and related data in the region 4.7°K to 14.7°K.

C. Temperature Measurement and Control

The liquid baths used were helium (1.2–5°K), hydrogen (14–24.5°K), and neon (24.5–31°K). Constant homogeneous temperature was effected by maintaining constant vapor pressure above the bath while stirring the bath with bubbles generated by a small heater at the bottom. In the helium region, temperatures were computed to 0.001° on the 1958 scale described by Van Dijk and Durieux (*21*). In the other regions, temperatures were computed to 0.001° on the scales used previously in the melting curve determinations (*1*).

D. Volume Calibrations

The volume of the large, thin-walled cell was determined to be 0.48252 cm^3 at 300°K and 1 atmos from the weight of mercury required to fill it. As indicated previously (*15*), corrections to the volume were made for: (1) the decrease

caused by insertion of the inlet capillary; (2) the contraction with decrease in temperature; and (3) the expansion with increase in pressure. Dead volumes in the system were measured by simple gas expansion.

E. Corrections

The various corrections discussed earlier (*15*) were applied to the present measurements. For dead-volume calculations, present data on He^3 and He^4 gas densities at room temperature were used at pressures up to 200 kg cm^2. From 200 to 1000 kg cm^2 the He^4 gas densities of Wiebe *et al.* (*22*) at room temperature were used. Above 1000 kg cm^2 an extrapolation of their data was made using as a guide the results of Bridgman (*23*) on impure He^4.

Following each ΔV_m determination, when the cell valve was reopened to the free piston gauge, movement of the piston indicated that either too little or too much gas had been bled into the metering system. The amount of excess or deficient gas was calculated from observation of the piston travel.

Compressibility of the gas at room temperature in the inlet capillary was calculated (*22*) and subtracted from the observed compressibilities in order to arrive at the true compressibility of fluid in the cell. This correction was calculable to <1 percent error and in magnitude was about 10 percent of the measured ΔV.

To effect freezing and melting, finite subcooling and superheating, respectively, were required (*15*). Corrections for these were made using the measured ΔT's the measured α_f, and α_s estimated as $0.75\ \alpha_f$. The ΔT used in freezing amounted to 0.03–1.2° for He^4 and 0.05–1.0° for He^3; the ΔT used in melting was 0.04–0.40° for He^4 and 0.04–0.21° for He^3. Small ΔT's were usually satisfactory with the thin-walled cell, although large ΔT's were occasionally used.

III. RESULTS

For both helium isotopes, experimental measurements of the volume change on melting, ΔV_m, are shown graphically as a function of melting pressure up to 3500 kg/cm^2 in Fig. 1. The data below 250 kg cm^2 are shown in more detail in Fig. 2. Values of the thermal expansion coefficient of the fluid,

$$\alpha_f = 1/V_f(\partial V_f/\partial T)_P ,$$

along the melting curve are plotted in Fig. 3. For He^3 a more detailed plot of α_f at low pressures and a plot of the fluid compressibility coefficient,

$$\beta_f = -1/V_f(\partial V_f/\partial P)_T ,$$

along the melting curve are shown in Fig. 4. The error in each of α_f and β_f is estimated to be ±5 percent. Figure 5 gives the locus of points in the pressure-temperature diagram for He^3 where the thermal expansion coefficient of the

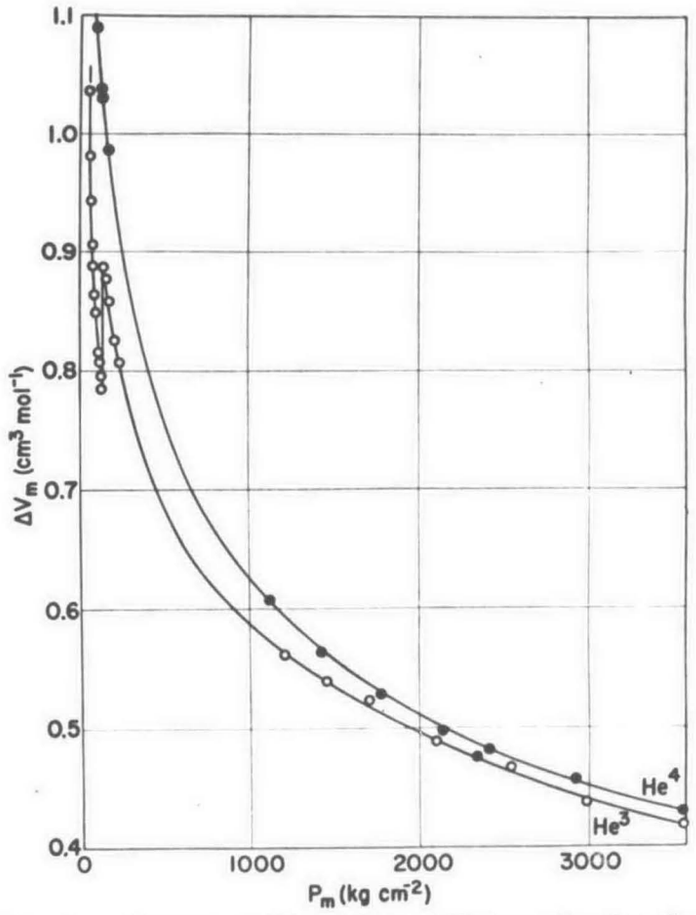

FIG. 1. The volume change on melting of He^3 and He^4 as a function of pressure.

fluid is zero. In Figs. 6 and 7 are plotted the values of $(\partial\alpha_f/\partial T)_P$ and $(\partial\beta_f/\partial P)_T$, respectively, for He^3 along the melting curve. Also shown in Fig. 6 are $(\partial\alpha_f/\partial T)_P$ values for the $\alpha_f = 0$ points of Fig. 5. For He^4 at temperatures below the lambda temperature, a plot of α_f versus T at $P = 25.47$ kg cm^{-2} is shown in Fig. 8. Figure 9 is the condensed phase diagram for He^3, showing the solid $\alpha \rightarrow$ solid β transition line (extrapolated to $T = 0$) and the $\alpha_f = 0$ locus in the liquid domain. Deviations of the individual experimental points from the curves of Fig. 9 are not visible on the scale.

The experimental and derived melting properties of He^4 are presented at various melting points in Table I. Values of ΔS_m were computed from ΔV_m and

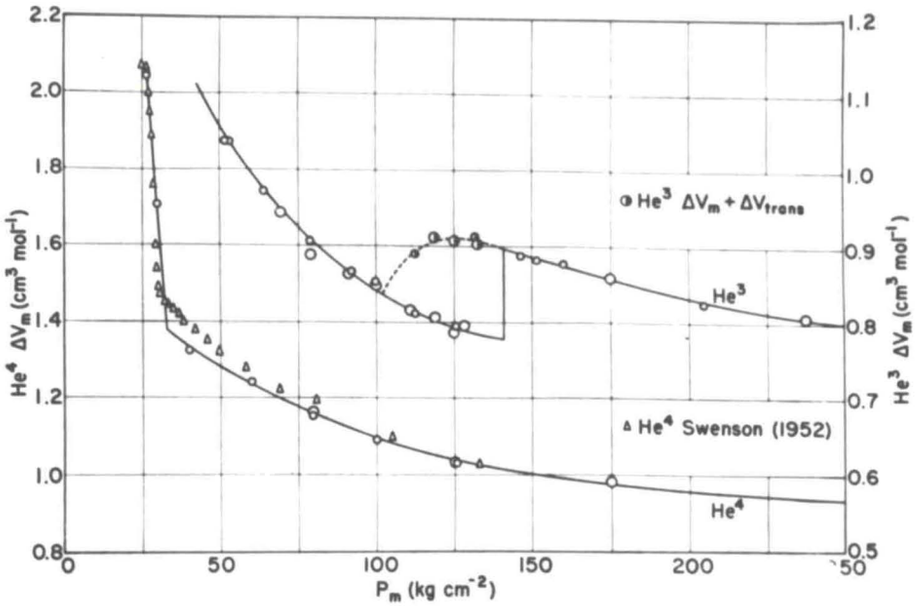

FIG. 2. The volume change on melting of He^3 and He^4 at low pressures. The large circles represent measurements made with the small, heavy-walled cell, while the small circles represent those made with the large, thin-walled cell.

dP_m/dT_m. Similar properties for He^3 are given in Table II. Maximum errors are estimated to be 0.5 percent for ΔV_m, 0.1 percent for V_f, and 1 percent for ΔS_m. In Table III are presented the melting parameters for the solid-solid transition of He^3. Results of the high-pressure, room-temperature gas-density determinations for He^4 and He^3 are given in Table IV.

As in the case of N_2 (*15*), the ΔV_m data were fitted to the equation

$$\Delta V_m = A - B \log_{10}(P_m + C) \tag{1}$$

by the method of least squares. For He^3 two sets of constants were needed—one for the region below the triple point and the other for the region above. It was not possible to fit the He^4 ΔV_m data to Eq. (1) over the full pressure range studied. However, for the purpose of interpolation, a fit was made from 175 to 3555 kg/cm^2. The constants in Eq. (1) for the various solids are presented in Table V. Listed also are the pressure range and rms deviation in ΔV_m.

The melting curve data at low pressure were fitted by the method of least squares to analytical expressions of the form,

$$P = A' + B'T + C'T^2 + D'T^3 + E'T^4. \tag{2}$$

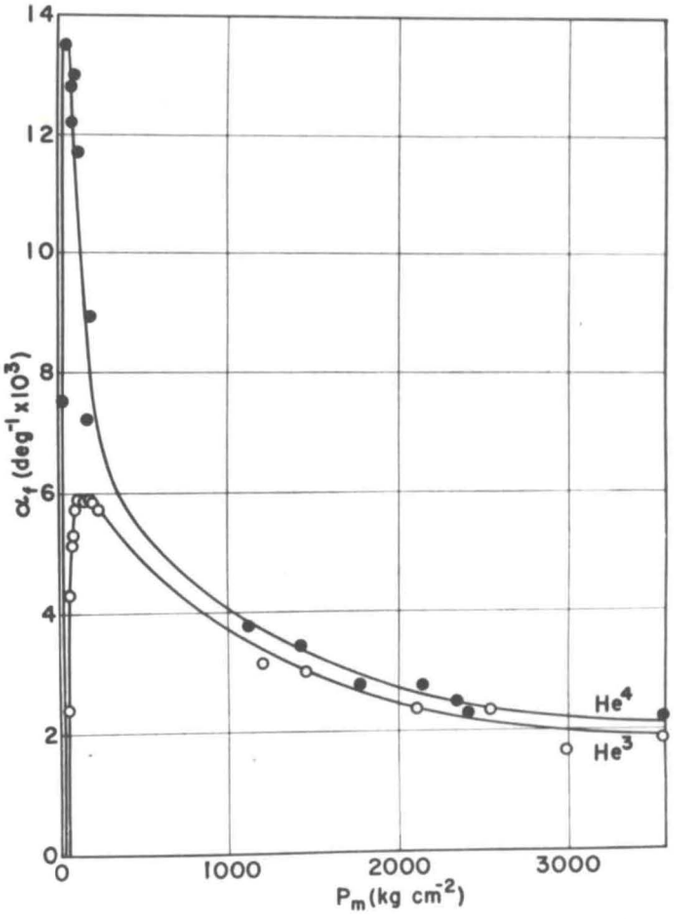

FIG. 3. The thermal expansion coefficient of fluid He^3 and He^4 along the melting curve.

For He^4 a fit was made only above the λ-point; for He^3 separate curves were fitted below and above the triple point. Fitted also to this equation were measurements of the solid-solid transition line in He^3. Constants in Eq. (2) for the various transitions are given in Table VI along with the temperature range covered and the rms deviation in P. The melting curves at higher temperatures and pressures are well represented by the constants given earlier (*1*) for the Simon equation,

$$P_m = a + bT_m^c. \tag{3}$$

Data for the molar volume of fluid along the melting curve could be repre-

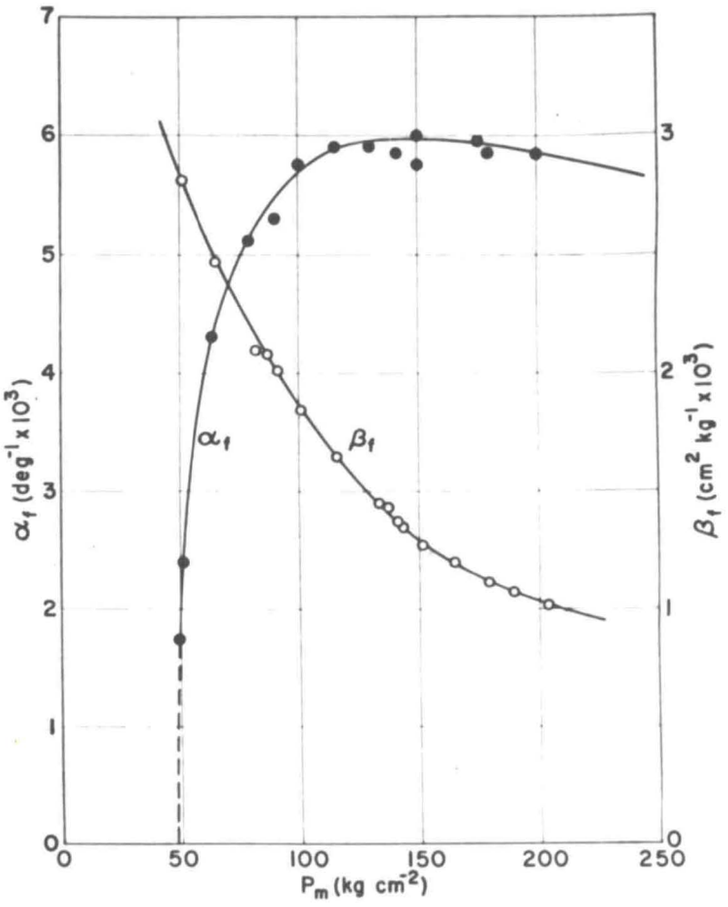

FIG. 4. The thermal expansion coefficient, α_f, and the compressibility coefficient, β_f, of fluid He^3 along the melting curve.

sented by an equation of the type

$$V_f = d' + b'(P_m + a')^{c'}. \tag{4}$$

A similar equation, with $d' = 0$, had been used for N_2 measurements (*15*). The constants of Eq. (4), obtained by a least-squares fit of the experimental data for He^4 and He^3, are given in Table VII together with the range of applicability and rms deviation in V_f. Equation (4) applied to He^3 and He^4 I probably does not fully reflect the accuracy of the measurements but is useful in making interpolations.

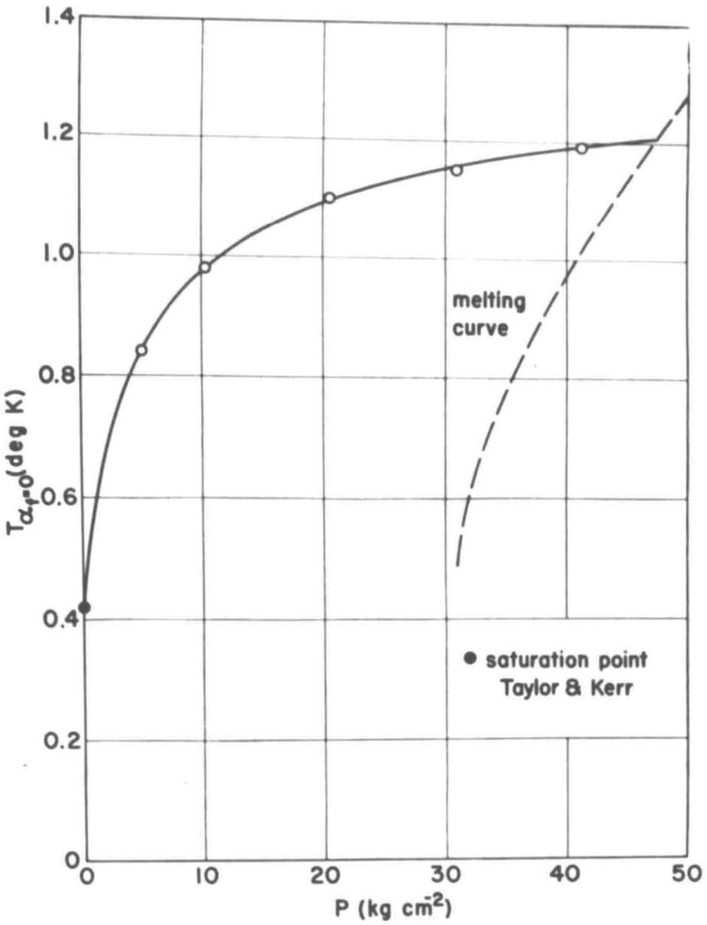

FIG. 5. Pressure-temperature diagram of $\alpha_f = 0$ for fluid He^3.

IV. DISCUSSION

A. Discussion of He^4 Results

Values of ΔV_m derived from molar volumes of solid and fluid measured by Dugdale and Simon (3), agree within 2 percent with the present determinations at pressures below 300 kg/cm^2 and above 2000 kg/cm^2. At intermediate pressures, however, their values are consistently lower than those reported here. A maximum deviation of -7 percent occurs at 1000 kg/cm^2.

Below 250 kg cm^2 a plot of the present ΔV_m data in Fig. 2 shows a sharp break in the curve at about 32 kg cm^2, corresponding to a melting temperature of

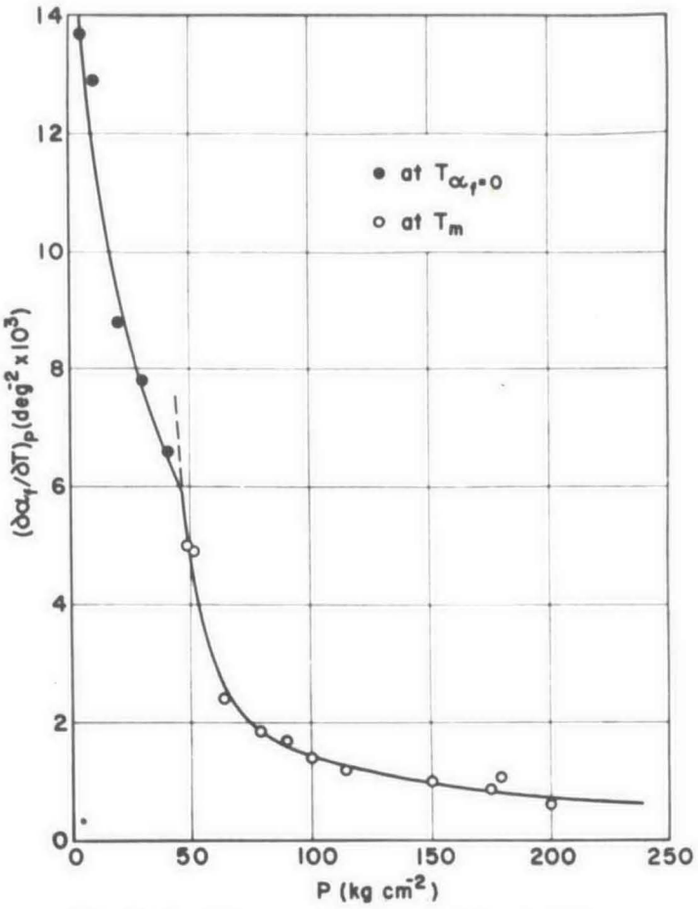

FIG. 6. $(\partial\alpha_f/\partial T)_P$ as a function of P for fluid He^3.

1.8°K. Although these values are somewhat higher than the more accurate, directly determined values (31 kg cm^2 and 1.77°K) of Swenson (*5*) and Keesom and Keesom (*9*) for $P_{m\lambda}$ and $T_{m\lambda}$, the point where the lambda line intersects the melting curve, the discontinuity in slope in ΔV_m is quite definite. The results of Swenson (*6*) are plotted also in Fig. 2. They show a positive deviation from the present values at $P_m > P_{m\lambda}$ and a negative deviation at $P_m < P_{m\lambda}$. The maximum deviation is about 5 percent in the vicinity of $P_{m\lambda}$. Swenson made no corrections to his ΔV_m measurements to account for the thermal expansion of solid and fluid over the ΔT region in which he worked; he assumed equilibrium in freezing and melting. With decreasing P_m the thermal expansion co-

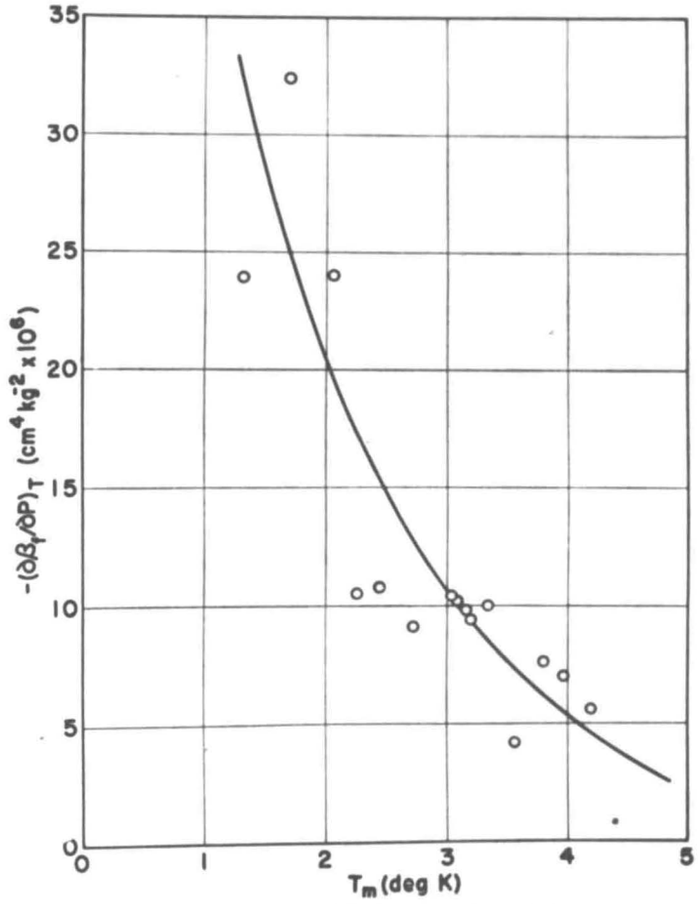

FIG. 7. $(\partial\beta_f/\partial P)_T$ for fluid He^3 along the melting curve.

efficient of the liquid changes from a positive value to a large negative value at $P_{m\lambda}$ (see, for example, Figs. 3 and 8). It is suggested that if expansion corrections were applied to Swenson's data, the break in his ΔV_m curve would be much sharper and in closer agreement with the present curve. The indirect ΔV_m data of Keesom and Keesom (*9*) from 46 to 133 kg/cm^2 have not been plotted in Fig. 2, but their ΔV_m curve would cross the present one at about 110 kg/cm^2, exhibiting maximum deviations of +9 percent at 46 kg/cm^2 and −6 percent at 123 kg/cm^2.

Each value of α_f along the melting curve was determined from a series of measurements made at constant pressure and extrapolated to the melting tem-

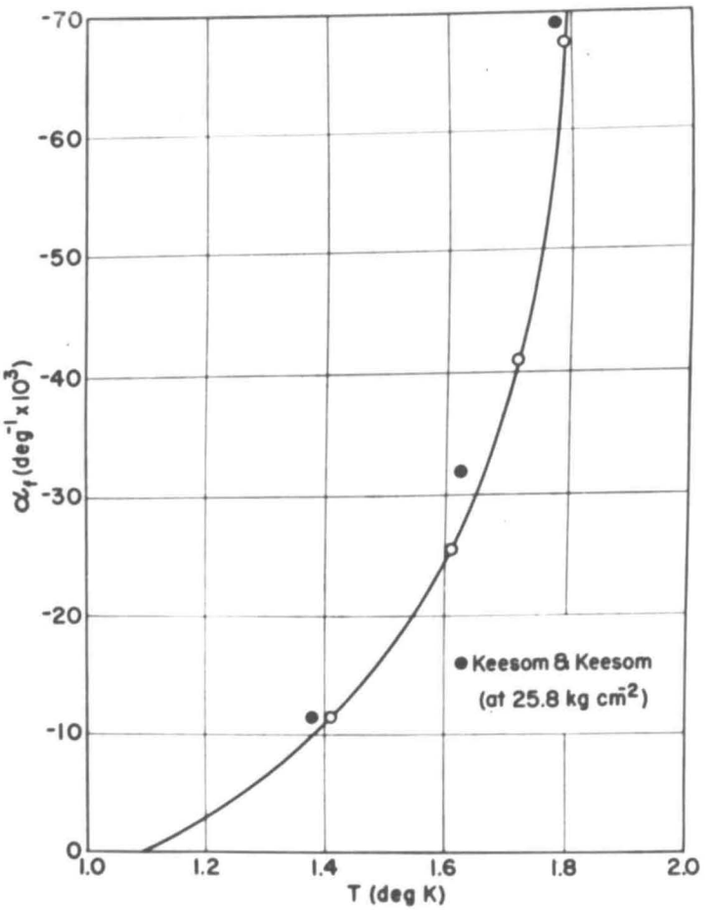

FIG. 8. α_f as a function of T for He^3 at $P = 25.47$ kg cm^{-2} and $T < T_\lambda$.

perature. The curve of Fig. 3 exhibits a sharp rise in α_f with decreasing P_m until a maximum is reached at ~ 50 kg cm^{-2}. At pressures below this, α_f decreases rapidly, becomes discontinuous at the λ-point by assuming large negative values which decrease in magnitude with further decreases in P_m, as shown in Fig. 8. The α_f values of Keesom and Keesom (*9*), plotted in Fig. 8, were derived from their PVT measurements and show good agreement with the present data.

The V_f measurements of Table I agree with those of Dugdale and Simon (*3*) to within 1 percent. The newly determined melting curve, expressed by Eq. (2) and Table VI, forms a smooth extension of that reported earlier (*1*).

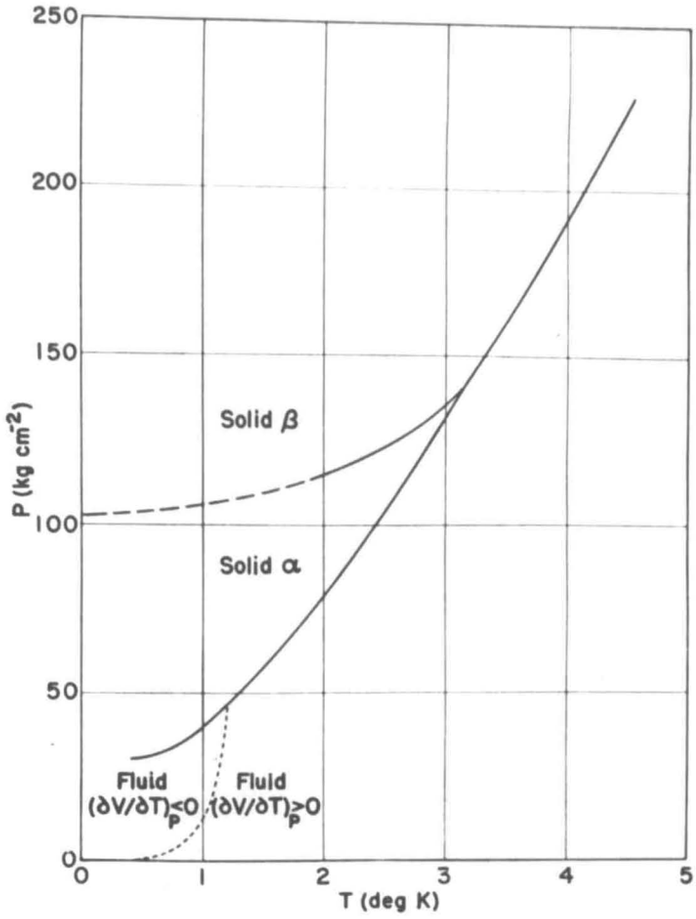

FIG. 9. Condensed phase diagram for He^3.

B. Discussion of He^3 Results

At high pressures the properties of He^3 along the melting curve roughly parallel those of He^4. At low pressures, although He^3 does not display superfluidity, there are other unique features which merit detailed discussions.

1. The solid-solid transition

With reference to Fig. 2, the discontinuity in the ΔV_m curve for He^3 at ~ 141 kg/cm^2 is a consequence of a triple point in the melting curve where two types of solid are in equilibrium with the fluid phase. A careful determination of the melting curve showed a slight discontinuity in slope which occurs at 141 kg/cm^2

TABLE I

PROPERTIES OF He^4 ALONG THE MELTING CURVE

P_m (kg/cm²)	T_m (°K)	ΔV_m (cm³/mol)	n[a]	Av. dev.[b] (±%)	V_f (cm³/mol)	ΔS_m[c] (cal/deg/mol)
26.48	1.350	2.046[d]	4	0.32	23.030[d]	0.170
29.88	1.723	1.706[d]	4	1.59	22.448[d]	0.840
40.00	2.046	1.324[d]	2	0.53	21.507[d]	1.142
60.02	2.540	1.241[d]	3	1.70	20.495[d]	1.260
78.95	2.943	1.152[d]	5	0.72	19.745	1.316
79.04	2.947	1.164	3	1.06	19.741	1.316
99.99	3.355	1.089[d]	2	0.25	19.104	1.350
125.21	3.835	1.038	4	0.85	18.489	1.374
125.47	3.840	1.029[d]	2	0.85	18.485	1.374
175.05	4.688	0.986	3	1.42	17.573	1.402
1120.3	14.746	0.6073	5	0.46	12.752	1.704
1422.8	17.158	0.5630	4	0.21	12.173	1.724
1778.6	19.774	0.5277	5	0.25	11.666	1.746
2134.2	22.210	0.4970	3	0.40	11.225	1.764
2347.7	23.602	0.4752	3	0.21	11.031	1.774
2417.8	24.050	0.4814	3	0.10	10.974	1.777
2930.1	27.190	0.4567	3	0.34	10.512	1.798
3555.6	30.770	0.4300	2	0.55	10.115	1.820

[a] n = number of ΔV_m determinations at each P_m.

[b] The average deviation from the mean of the n determinations of ΔV_m.

[c] Smoothed values.

[d] Results with the large cell; all others with the small cell.

and 3.16°K, the point of intersection of the two limbs of the melting curve. Probably a more accurate determination is given by the intersection of the solid-solid transition line with the melting curve, which occurs at 140.44 kg/cm² and 3.148°K.

Subsequent to these measurements, the structures of the two solid forms of He^3 were determined by x-ray diffraction (*24*). The solid modification α, which exists at the lower temperatures and pressures, was found to have the body-centered-cubic structure. It was determined that the β modification has the hexagonal-closest-packed structure. Solid densities, derived from lengths of the axes of the unit cells, are in good agreement with densities computed from data reported here.

With reference again to Fig. 2, a half-shaded circle represents the sum of the volume change on melting of α-solid plus the volume change of the solid-solid transition, ΔV_{trans}, at a given pressure. These results were obtained by the usual technique for measuring ΔV_m except that the bath temperature was low enough to cause freezing of β-solid. The difference between the upper dashed curve of

TABLE II

PROPERTIES OF He^3 ALONG THE MELTING CURVE

P_m (kg/cm²)	T_m (°K)	ΔV_m (cm³/mol)	n[a]	Av. dev.[b] (±%)	V_f (cm³/mol)	ΔS_m[c] (cal/deg/mol)
			α-solid			
51.61	1.332	1.0366[d]	2	0.45	23.700[d]	0.842
53.17	1.375	1.0360[d]	1	—	23.575	0.856
64.06	1.659	0.9700[d]	2	0.20	22.767[d]	0.930
69.28	1.783	0.9435	2	0.11	22.450	0.955
78.95	1.998	0.9060[d]	1	—	21.920[d]	0.988
79.00	2.000	0.8880	4	0.72	21.917	0.988
91.27	2.255	0.8633	2	0.97	21.360	1.018
92.08	2.272	0.8656[d]	2	0.28	21.330	1.020
99.94	2.425	0.8523[d]	1	—	21.015	1.033
100.00	2.427	0.8488	3	1.64	21.012	1.033
110.86	2.630	0.8153	3	0.55	20.625	1.048
112.42	2.658	0.8107[d]	4	1.06	20.575	1.049
118.85	2.775	0.8063	3	2.88	20.355	1.056
125.16	2.887	0.7856	2	0.15	20.152	1.060
125.41	2.893	0.7954[d]	2	0.53	20.145	1.061
128.40	2.943	0.7955	2	0.36	20.055	1.063
			β-solid			
146.29	3.252	0.8868[d]	4	0.56	19.543	1.186
151.51	3.343	0.8816[d]	2	0.84	19.417	1.193
160.13	3.490	0.8766[d]	2	0.16	19.230	1.204
175.01	3.735	0.8583	5	0.50	18.935	1.223
204.57	4.205	0.8250[d]	3	1.15	18.388	1.259
237.43	4.732	0.8066	5	0.46	17.848	1.299
1208.8	14.689	0.5617	2	0.02	12.991	1.617
1449.2	16.592	0.5394	2	0.53	12.511	1.648
1707.2	18.518	0.5231	2	0.36	12.123	1.669
2098.6	21.256	0.4880	3	0.08	11.595	1.695
2543.0	24.158	0.4664	3	0.13	11.140	1.714
2986.8	26.887	0.4373	3	0.14	10.800	1.727
3554.8	30.184	0.4179	3	0.58	10.398	1.738

[a] n = number of ΔV_m determinations at each P_m.

[b] The average deviation from the mean of the n determinations of ΔV_m.

[c] Smoothed values.

[d] Results with the large cell; all others with the small cell.

Fig. 2 and the lower solid curve gives ΔV_{trans}. The dotted curve appears to hook over, and one can speculate that it intersects the solid curve at ~102 kg cm^{-2} at which point ΔV_{trans} is zero. It is interesting to note that the solid transition curve of Fig. 9 seems to extrapolate to about this same pressure at 0°K and to exhibit a zero slope. As shown in Table III, ΔS_{trans} approaches zero at a faster rate than ΔV_{trans}.

TABLE III

PROPERTIES[a] OF THE TRANSITION IN SOLID He^3, $\beta \rightleftharpoons \alpha$

P (kg/cm²)	T (°K)	dP/dT (kg/cm²/deg)	ΔV (cm³/mol)	ΔS (cal/deg/mol)
140.44[b]	3.148[b]	34.0	0.116	0.092
130	2.805	27.0	0.118	0.074
120	2.370	19.2	0.100	0.045
112	1.846	11.6	0.072	0.019

[a] Smoothed values.

[b] Triple point for solid α, β, and fluid.

TABLE IV

GAS DENSITIES OF He^3 AND He^4 AT 24.40°C

P kg/cm²	ρ He^4 Amagats	ρ He^3 Amagats
53.44	46.30	46.28
112.45	94.95	94.81
204.55	166.20	165.99

TABLE V

CONSTANTS[a] IN EQ. (1) FOR THE VOLUME CHANGE OF MELTING

Solid	A	B	C	P_m range, kg/cm²	rms dev. cm³/mol
He^4	1.60677	0.33439	−103.25	175 3555	0.0051
He^3 α	1.56464	0.39023	−29.998	51 128	0.0064
He^3 β	1.51053	0.30825	−42.581	146 3555	0.0031

[a] Pressure units in kg/cm² and volume units in cm³/mol.

TABLE VI

CONSTANTS[a] IN EQ. (2) FOR THE VARIOUS TRANSITIONS

Transition	A'	B'	C'	D'	E'	T range, deg K	rms dev., kg/cm²
Solid He^4 → fluid He^4 I	33.280	−44.156	31.799	−4.8159	0.30313	1.8 5.2	0.23
Solid He^3 α → fluid	27.256	−0.64696	16.0205	−1.39505	0	1.2 3.1	0.16
Solid He^3 β → fluid	3.873	30.5539	4.08176	0	0	3.2 4.4	0.10
Solid He^3 α → Solid He^3 β	104.906	0	−0.053454	1.15635	0	1.8 3.1	0.42

[a] Pressure units in kg/cm² and temperature units in deg K.

TABLE VII

CONSTANTS[a] IN EQ. (4) FOR MOLAR VOLUMES OF FLUID ALONG THE MELTING CURVE

Fluid	a'	b'	c'	d'	P_m range, kg/cm²	rms dev., cm³/mol
He^4 II	0	−0.17145	1	27.570	26–30	0.0006
He^4 I	14.854	48.5273	−0.107253	−10.0712	35–3555	0.0097
He^3	1.075	51.1102	−0.161532	−3.2482	50–3555	0.0137

[a] Pressure units in kg/cm² and volume units in cm³/mol.

2. Thermal expansion and compressibility of the fluid

The thermal expansion coefficient of fluid He^3 along the melting curve exhibits a maximum in the vicinity of the triple point, as shown in Figs. 3 and 4. The maximum is broad compared to that for He^4 and is less than one-half as large. In general, one expects α to increase with T and decrease with P; however, along the melting curve the "normal" behavior of α_f increasing with decreasing P_m and T_m indicates that P_m changes overcome T_m changes. For He^4 the maximum in α_f appears to be a direct consequence of the λ-transition. In He^3 the nuclear spin part of α_f becomes more negative at lower T, according to Goldstein (*25*), and it apparently overcomes the "normal" behavior of the nonspin part of α_f.

From values of α_f and β_f in Fig. 4, it is possible to compute the following thermodynamic quantities for fluid He^3 along the melting curve:

$$(\partial P_f/\partial T)_V = \alpha_f/\beta_f ; \tag{5}$$

and

$$(C_P - C_V) = TV_f\alpha_f^2\,\beta_f . \tag{6}$$

These quantities are shown as the curves in Fig. 10. Neither curve exhibits a maximum over the range studied. The plot of $(C_P - C_V)$ versus P_m is linear below 180 kg/cm² and extrapolates to zero at $P_m = 47$ kg/cm². This extrapolation gives a good determination of the point where α_f goes through zero on the melting curve.

The pressure-temperature locus of $\alpha_f = 0$ in the fluid domain is shown in Figs. 5 and 9. For completeness, the point of Taylor and Kerr (*26*) on the vaporization curve has been included.[3] The points represented by open circles were obtained by extrapolation to zero of a series of α_f values measured at constant pressure and various temperatures. This could be done reliably because the slopes were quite constant. Extrapolations were made below about 1.4°K, the

[3] Lee *et al.* (*27*) also reported a density maximum at approximately 0.5°K, presumably at saturation.

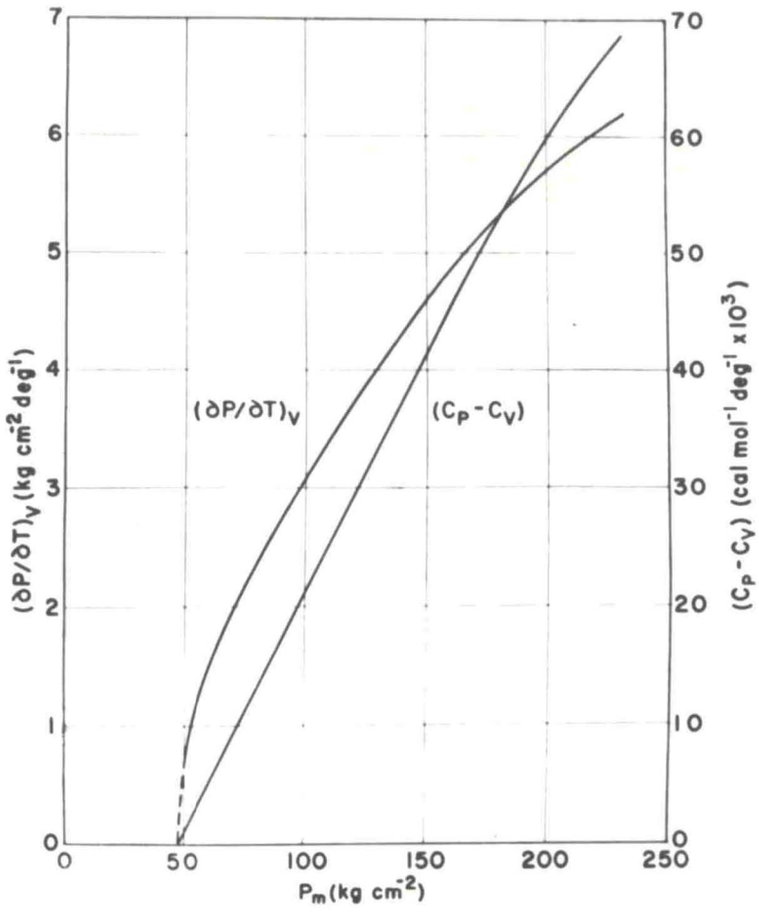

FIG. 10. $(\partial P/\partial T)_V$ and $(C_P - C_V)$ for fluid He^3 along the melting curve.

lowest accessible mean temperature for the present α_f measurements. It is seen that the curve of Fig. 5 intersects the melting curve at 47 kg cm^{-2} in good agreement with the extrapolations made in Figs. 4 and 10. Temperatures where $\alpha_f = 0$, derived from pressure-volume-temperature data by Brewer and Daunt (*28*) and Sherman and Edeskuty (*29*), are in general agreement with the measurements of Fig. 5.

The slopes, $(\partial\alpha_f/\partial T)_P$ and $(\partial\beta_f/\partial P)_T$, decrease with increasing melting pressure as shown in Figs. 6 and 7, respectively. From the thermodynamic formulas,

$$(\partial C_P/\partial P)_T = -T(\partial^2 V/\partial T^2)_P = -TV[\alpha^2 + (\partial\alpha/\partial T)_P] \qquad (7)$$

and the data given above for fluid He^3, it can be seen that C_P decreases with increasing pressure in the vicinity of the melting curve. Gutsche (*30*) and Jones and Walker (*31*) reported a similar variation for H_2 and A, respectively.

Equation (5) combined with the thermodynamic relation,

$$\frac{dP_m}{dT_m} = \left[\left(\frac{\partial P}{\partial V}\right)_T\right]_m \frac{dV_m}{dT_m} + \left[\left(\frac{\partial P}{\partial T}\right)_V\right]_m, \tag{8}$$

leads to

$$\beta_f = \alpha_f \frac{dT_m}{dP_m} - \frac{1}{V_f}\frac{dV_f}{dP_m}. \tag{9}$$

For He^3 at low pressures, the values of β_f calculated from Eq. (9) compare reasonably well with those measured directly (Fig. 4), deviating by +27 percent at $P_m = 50$ kg/cm^2 and by −2 percent at $P_m = 225$ kg/cm^2. At 3555 kg/cm^2, the calculated β_f is 7.4×10^{-5} cm^2/kg.

The theory of melting for metals that was advanced by Bonfiglioli *et al.* (*32*) predicts that $\alpha_s T_m$ is constant for a given crystal type. Unfortunately, available data are restricted to melting pressures of ~1 atmos but for face-centered-cubic, body-centered-cubic, and hexagonal-closest-packed metals of widely varying melting temperature, $\alpha_s T_m$ appears to be ~0.06. Above the anomalous region where α_f shows a maximum, the present results for fluid He^3 (and He^4) indicate that values of $\alpha_f T_m$ rise rapidly with P_m then approach constancy around 0.05–0.06 at high melting pressures. The empirical deduction from the present work that $\alpha_s = 0.75\alpha_f$ indicates that the expansion of the solid along the melting curve follows closely that of the fluid and implies a constant value of 0.04–0.05 for $\alpha_s T_m$ at high pressures. It is interesting to compare the ratio $\alpha_s/\alpha_f = 0.75$ for He^3 and He^4 with the ratios 0.70 and 0.77 for Na and K, respectively, measured by Bridgman (*33*) at $P_m = 1$ kg/cm^2.

Values of V_s can be calculated from the present measurements of V_f and ΔV_m. For He^3 the ratio V_f/V_s was found to be constant and equal to 1.044 with a maximum deviation of only 0.4 percent over the full pressure range studied.[4] Therefore $(1/V_f)(dV_f/dP_m) = (1/V_s)(dV_s/dP_m)$ which, with Eq. (8) and the ratio $\alpha_s/\alpha_f = 0.75$, leads to the following equations for He^3:

$$\beta_s = 0.75\alpha_f \frac{dT_m}{dP_m} - \frac{1}{V_f}\frac{dV_f}{dP_m}, \tag{10}$$

and

$$\Delta\beta = \beta_f - \beta_s = 0.25\alpha_f(dT_m/dP_m). \tag{11}$$

[4] For He^4 the ratio of V_f/V_s varied monotonically from 1.066 at $P_m = 35$ kg/cm^2 to 1.044 at $P_m = 3555$ kg/cm^2.

Experimental data substituted in the latter equation show that, over the range 50–225 kg/cm^2, $\Delta\beta$ has a constant value of $\sim 2.5 \times 10^{-5}$ cm^2/kg, which is at most 2.5 percent of β_f. At 3555 kg/cm^2 $\Delta\beta$ is calculated to be 2.8×10^{-6} cm^2/kg or 5 percent of β_f. The compressibility coefficient of solid He^3 is therefore very similar to that of the fluid along the full range of the melting curve investigated. For Na and K, the data of Bridgman (*34*) lead to values of 38 and 29 percent, respectively, for $\Delta\beta/\beta_f$ at $P_m = 1$ kg/cm^2.

C. Thermal Properties of Melting

At the lower end of the P_m range for He^3, the ΔS_m results were combined with the entropy of saturated liquid S_{sat}, measured by Roberts and Sydoriak (*35*), and the entropy of compression ΔS_{comp} to give the entropy of solid. The values of ΔS_{comp} can be obtained through the formula

$$\Delta S_{comp} = -\int_{P_{sat}}^{P_m} \left(\frac{\partial V}{\partial T}\right)_P dP.$$

For the computation, the present measurements were used from 5 kg cm^2 to P_m, and those of Sherman and Edeskuty (*29*), from P_{sat} to 5 kg cm^2. The results over 1.2° to 2.0°K showed the entropy of solid at the melting curve (or S_α) to rise only from 1.34 to 1.43 cal/deg/mol. Subtraction of the entropy change of compression and of transition in solid gave approximate S_β values of 1.32 to 1.34. The entropy associated with a nuclear spin system in completely random orientation is $S = R \ln 2 = 1.38$. It would appear that for solid He^3 this is the major source of entropy.

The values of ΔS_m listed in Tables I and II were derived from the Clapeyron equation using experimental ΔV_m data and slopes computed from analytical expressions for the melting curves. For both He isotopes ΔS_m increases with P_m over the experimental range covered, although the increase becomes progressively smaller at higher melting pressures. This behavior is contrary to that of N_2 (*15*), which showed a decrease of ΔS_m with increasing P_m. Ebert (*36*), using melting properties for almost all materials studied to 1947 by Bridgman, found that ΔS_m and ΔV_m always decrease with rising P_m and, indeed, extrapolate to zero at some finite high pressure, a criterion of a critical point. The behavior of He then appears to be anomalous, at least up to 3555 kg cm^2. The continued rise with pressure of ΔS_m is incompatible with the possibility of a critical point between solid and fluid. Since the question of a critical point in melting curves has yet to be resolved, it is interesting to extrapolate the He melting data to higher pressures than were measured.

An expression for ΔS_m at high pressures can be derived in terms of P_m by combining Eqs. (1) and (3). When $d\Delta S_m/dP_m$ is set equal to zero, one finds the solutions $P_m = 4219$ kg/cm^2 and $P_m = 3628$ kg/cm^2 for He^3 and He^4, respectively.

These melting pressures are only slightly higher than the present experimental range and represent pressures at which maxima occur in ΔS_m. At higher pressures ΔS_m decreases with P_m and finally extrapolates to zero at $P_m = 79{,}500$ kg/cm^2 ($T_m = 235°$K) for He^3 and $P_m = 63{,}900$ kg/cm^2 ($T_m = 197°$K) for He^4. Therefore, a critical point in the melting curve is not precluded by the available data. There is some indication that the melting thermal properties of the heliums become "normal" at sufficiently high pressures.

ACKNOWLEDGMENT

We wish to thank R. H. Sherman for assistance in fitting experimental data to analytical equations.

RECEIVED: March 23, 1959

REFERENCES

1. R. L. MILLS AND E. R. GRILLY, *Phys. Rev.* **99,** 480 (1955).
2. D. W. Osborne, B. M. Abraham, and B. Weinstock, *Phys. Rev.* **82,** 263 (1951); **85,** 158 (1952).
3. J. S. DUGDALE AND F. E. SIMON, *Proc. Roy. Soc.* **A218,** 268 (1953).
4. F. A. HOLLAND, J. A. W. HUGGILL, and G. O. JONES, *Proc. Roy. Soc.* **A207,** 268 (1951).
5. C. A. SWENSON, *Phys. Rev.* **89,** 538 (1953).
6. C. A. SWENSON, *Phys. Rev.* **86,** 870 (1952).
7. C. A. SWENSON, *Phys. Rev.* **79,** 626 (1950).
8. W. H. KEESOM AND J. H. C. LISSMAN, *Leiden Comm.* **232b** (1934).
9. W. H. KEESOM AND A. P. KEESOM, *Leiden Comm.* **221e** (1933).
10. W. H. KEESOM, "Helium," p. 210. Elsevier, Amsterdam, 1942.
11. F. SIMON, M. RUHEMANN, and W. A. M. EDWARDS, *Z. physik. Chem.* **B6,** 62 (1929), **B6,** 331 (1930).
12. F. SIMON, *Z. physik. Chem.* **B2,** 340 (1929).
13. F. E. SIMON AND C. A. SWENSON, *Nature* **165,** 829 (1950).
14. R. L. MILLS AND E. R. GRILLY, Proceedings of the Symposium on Liquid and Solid He^3, The Ohio State University, August 20–23, 1957, p. 100; Proceedings of the Fifth International Conference on Low Temperature Physics and Chemistry, University of Wisconsin, August 26–31, 1957, p. 106. Univ. of Wisconsin Press, Madison, 1958.
15. E. R. GRILLY AND R. L. MILLS, *Phys. Rev.* **105,** 1140 (1957).
16. O. C. BRIDGEMAN, *J. Am. Chem. Soc.* **49,** 1174 (1927).
17. C. H. MYERS AND R. H. JESSUP, *J. Research Natl. Bur. Standards* **6,** 1061 (1931).
18. R. L. MILLS, *Rev. Sci. Instr.* **27,** 332 (1956).
19. S. G. SYDORIAK AND T. R. ROBERTS, Proceedings of the Fifth International Conference on Low Temperature Physics and Chemistry, University of Wisconsin, August 26–31, 1957, p. 212. Univ. of Wisconsin Press, Madison, 1958.
20. R. L. MILLS AND E. R. GRILLY, *Phys. Rev.* **101,** 1246 (1956).
21. H. VAN DIJK AND M. DURIEUX, *Physica* **24,** 920 (1958); *Leiden Comm. Suppl.* **115a**.
22. R. WIEBE, V. L. GADDY, AND C. HEINS, *J. Am. Chem. Soc.* **53,** 1721 (1931).
23. P. W. BRIDGMAN, *Proc. Am. Acad. Arts Sci.* **59,** 173 (1924).
24. A. F. SCHUCH, E. R. GRILLY, AND R. L. MILLS, *Phys. Rev.* **110,** 775 (1958).
25. L. GOLDSTEIN, *Phys. Rev.* **112,** 1483 (1958).

26. R. D. TAYLOR AND E. C. KERR, reported at the Kamerlingh Onnes Conference on Low Temperature Physics, Leiden, June 23–28, 1958.
27. D. M. LEE, J. D. REPPY, AND H. A. FAIRBANK, *Bull. Am. Phys. Soc.* Ser. II, **3,** 339 (1958).
28. D. F. BREWER AND J. G. DAUNT, *Bull. Am. Phys. Soc. Ser. II*, **4,** 6 (1959).
29. R. H. SHERMAN AND F. J. EDESKUTY, private communication.
30. H. GUTSCHE, *Z. physik. Chem.* **A184,** 45 (1939).
31. G. O. JONES AND P. A. WALKER, *Proc. Phys. Soc.* **B69,** 1348 (1956).
32. G. BONFIGLIOLI, A. FERRO, AND G. MONTALENTI, Changements de Phases Conference, Paris, June 2–7, 1952. Société de Chimie Physique, Paris, 1952.
33. P. W. BRIDGMAN, *Proc. Nat. Acad. Sci. U.S.* **21,** 109 (1935).
34. P. W. BRIDGMAN, *Phys. Rev.* **6,** 100 (1915).
35. T. R. ROBERTS AND S. G. SYDORIAK, *Phys. Rev.* **98,** 1672 (1955).
36. L. EBERT, *Österr. Chem.-Ztg.* No. 1/2, 1 (1954).